Rapid Communications

High baryon and energy densities achievable in heavy-ion collisions at $\sqrt{s_{NN}} = 39$ GeV

Yu. B. Ivanov[1,2,3,*] and A. A. Soldatov[2]

[1]*National Research Centre "Kurchatov Institute," Moscow 123182, Russia*

[2]*National Research Nuclear University "MEPhI," Moscow 115409, Russia*

[3]*Bogoliubov Laboratory of Theoretical Physics, JINR, Dubna 141980, Russia*

(Received 15 November 2017; revised manuscript received 8 January 2018; published 14 February 2018)

Baryon and energy densities, which are reached in central Au+Au collisions at collision energy of $\sqrt{s_{NN}} = 39$ GeV, are estimated within the model of three-fluid dynamics. It is shown that the initial thermalized mean proper baryon and energy densities in a sizable central region approximately are $n_B/n_0 \approx 10$ and $\varepsilon \approx 40$ GeV/fm^3, respectively. The study indicates that the deconfinement transition at the stage of interpenetration of colliding nuclei makes the system quite opaque. The final fragmentation regions in these collisions are formed not only by primordial fragmentation fireballs, i.e., the baryon-rich matter passed through the interaction region (containing approximately 30% of the total baryon charge), but also by the baryon-rich regions of the central fireball pushed out to peripheral rapidities by the subsequent almost one-dimensional expansion of the central fireball along the beam direction.

DOI: 10.1103/PhysRevC.97.021901

At ultrarelativistic energies, colliding nuclei pass through each other, compressing and depositing energy in each other, rather than mutually stopping, as at lower energies. The net-baryon charge remains concentrated in the fragmentation regions that are well separated in the configuration and momentum space from the midrapidity fireball. Properties of these baryon-rich fragmentation regions (i.e., the baryonic fireballs) produced in central heavy-ion collisions were discussed long ago [1–5]. A recent proposal [6] to perform experiments at the Large Hadron Collider (LHC) at CERN in the fixed-target mode (AFTER@LHC experiment) revived interest to the fragmentation regions. This experiment would provide an opportunity to carry out precision measurements in the kinematical region of the target fragmentation region. If the LHC operates in a fixed-target mode at a beam energy of 2.76 GeV per nucleon, this is equivalent to $\sqrt{s_{NN}} = 72$ GeV in terms of the center-of-mass energy. This energy is only slightly above the range of the Beam Energy Scan (BES) program at the BNL Relativistic Heavy Ion Collider (RHIC).

Recently theoretical considerations on the internal properties of baryonic fireballs were updated in Ref. [7] based on the McLerran-Venugopalan model [8]. It was argued [7] that in central Au+Au collisions at the top RHIC energy, high baryon densities (an order of magnitude greater than the normal nuclear one) over a large volume are achieved in fireballs outside the central-rapidity region. This is in contrast to almost net-baryon-free matter produced in the midrapidity region. However, the LHC energy in the fixed-target mode provides only $\sqrt{s_{NN}} = 72$ GeV, which is already near the lower limit of applicability of the McLerran-Venugopalan model [7]. Therefore, phenomenological approaches are required for estimation of the baryon and energy densities reached in the fragmentation regions at these energies.

In the present paper we estimate the baryon and energy densities reached in central Au+Au collisions within the model of three-fluid dynamics (3FD) [9,10]. The estimation is done for the highest collision energy of 39 GeV accessible for the 3FD simulations. This energy is certainly lower than the top LHC energy in the fixed-target mode; however, the main features of the fragmentation regions are expected to be similar to those at 72 GeV. The 3FD model is quite successful in reproducing the major part of the observables in the midrapidity region at the BES RHIC energies [10–16]. Therefore, the 3FD predictions for the fragmentation regions may be of interest.

Unlike conventional hydrodynamics, where local instantaneous stopping of projectile and target matter is assumed, a specific feature of the 3FD description [9] is a finite stopping power resulting in a counter-streaming regime of leading baryon-rich matter. This generally nonequilibrium regime of the baryon-rich matter is modeled by two interpenetrating baryon-rich fluids initially associated with constituent nucleons of the projectile (p) and target (t) nuclei. In addition, newly produced particles, populating the midrapidity region, are associated with a fireball (f) fluid. Each of these fluids is governed by conventional hydrodynamic equations coupled by friction terms in the right-hand sides of the Euler equations. These friction terms describe energy-momentum loss of the baryon-rich fluids. A part of this loss is transformed into thermal excitation of these fluids, while another part gives rise to particle production into the fireball fluid.

Friction forces between fluids are the key constituents of the model that determine dynamics of the nuclear collision. The friction forces in the hadronic phase were estimated in Ref. [17]. Precisely these friction forces are used in the simulations for the hadronic phase. There are no theoretical

*Y.Ivanov@gsi.de

estimates of the friction in the quark-gluon phase (QGP) so far. Therefore, the friction in the QGP is purely phenomenological. It was fitted to reproduce baryon stopping at high collision energies within the deconfinement scenarios, as is described in Ref. [10] in detail.

The physical input of the present 3FD calculations is described in Ref. [10]. The simulations in [10–16] were performed with different equations of state (EOSs)—a purely hadronic EOS [18] and two versions of the EOS involving the deconfinement transition [19], i.e., a first-order phase transition and a smooth crossover one. In the present paper we demonstrate results with only these deconfinement EOSs as the most successful in reproduction of various observables at high collision energies: the baryon stopping [10,11], yields of various hadrons [12], their mean transverse masses [13,14], the elliptic flow [15], etc. A detailed comparison with the recent STAR data on bulk observables [20] is presented in Ref. [16]. Due to numerical reasons [9], 39 GeV is the highest energy attainable for computations within the 3FD model.

For the discussion below we need to introduce some quantities. Within the 3FD model the system is characterized by three hydrodynamical velocities, u^μ_α with $\alpha =$ p, t, and f, attributed to these fluids. The interpenetration of the p and t fluids takes place only at the initial stage of the nuclear collision. At later stages either a complete mutual stopping occurs and these fluids get unified or these fluids become spatially separated. Therefore, we define a collective 4-velocity of the baryon-rich matter associating it with the total baryon current $u^\mu_B = J^\mu_B/|J_B|$, where $J^\mu_B = n_{\rm p}u^\mu_{\rm p} + n_{\rm t}u^\mu_{\rm t}$ is the baryon current defined in terms of proper baryon densities n_α of these fluids and hydrodynamic 4-velocities u^μ_α, and

$$|J_B| = (J^\mu_B J_{B\mu})^{1/2} \equiv n_B \tag{1}$$

is the proper (i.e., in the local rest frame) baryon density of the p and t fluids. In particular, this proper baryon density allows us to construct a simple fluid unification measure

$$1 - \frac{n_{\rm p} + n_{\rm t}}{n_B}, \tag{2}$$

which is zero when the p and t fluids are mutually stopped and unified, and has a positive value increasing with the rise of the relative velocity of the p and t fluids.

The total proper energy density of all three fluids in the local rest frame, where the composed matter is at rest, is defined as follows:

$$\varepsilon = u_\mu T^{\mu\nu} u_\nu. \tag{3}$$

This proper energy density is defined in terms of the total energy-momentum tensor $T^{\mu\nu} \equiv T^{\mu\nu}_{\rm p} + T^{\mu\nu}_{\rm t} + T^{\mu\nu}_{\rm f}$ being the sum of conventional hydrodynamical energy-momentum tensors of separate fluids, and the total collective 4-velocity of the matter

$$u^\mu = u_\nu T^{\mu\nu}/(u_\lambda T^{\lambda\nu} u_\nu). \tag{4}$$

Note that definition (4) is, in fact, an equation determining u^μ. In general, this u^μ does not coincide with 4-velocities of separate fluids. This definition is in the spirit of the Landau-Lifshitz approach to viscous relativistic hydrodynamics.

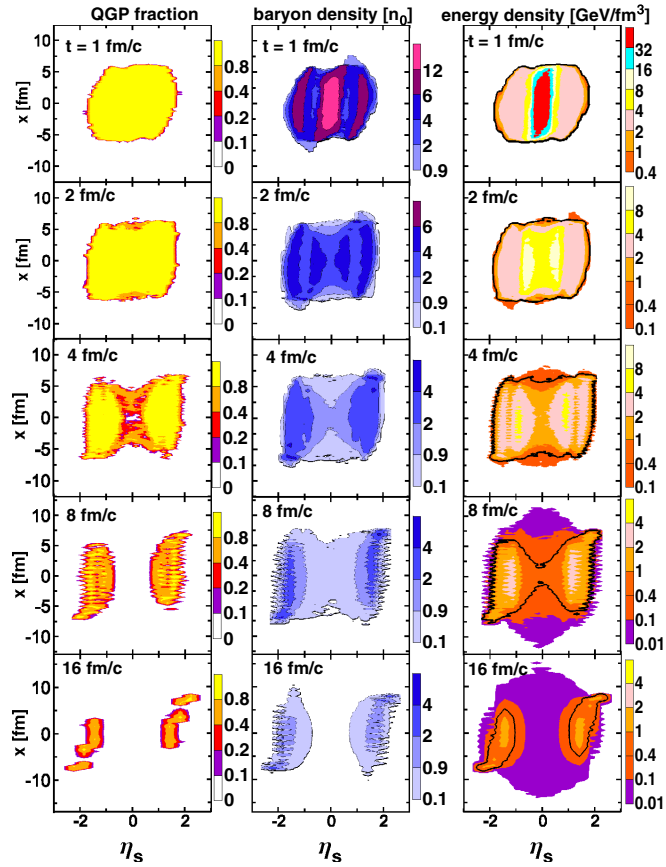

FIG. 1. QGP fraction (left column), the proper baryon density in units of the normal nuclear density, $n_0 = 0.15$ 1/fm^3, see Eq. (1) (middle column), and proper energy density, see Eq. (3) (right column), in the reaction plain $(x\eta_s)$ at various time instants (in the c.m. frame) in the central ($b = 2$ fm) Au+Au collision at $\sqrt{s_{NN}} = 39$ GeV. η_s is the space-time rapidity along the beam direction. Calculations are done with the first-order-transition EOS. The bold contours in panels of the right column display the borders between the frozen-out and still hydrodynamically evolving matter.

Figure 1 presents the time evolution of the QGP fraction and the proper baryon and energy densities, Eqs. (1) and (3), respectively, in the reaction plain $(x\eta_s)$ of central Au+Au collisions at $\sqrt{s_{NN}} = 39$ GeV, where

$$\eta_s = \frac{1}{2}\ln\left(\frac{t+z}{t-z}\right) \tag{5}$$

is the space-time rapidity and z is the coordinate along the beam direction. The baryon-rich fluids are mutually stopped and unified already at $t \gtrsim 1$ fm/c because the fluid unification measure, see Eq. (2), is practically zero (less than 0.02). The baryon-fireball relative velocity is small, $v_{fB} \lesssim 0.1$, at $t \geqslant 1$ fm/c. This indicates that a system is close to the thermal (kinetic) equilibrium. As the the f fluid is not that well unified with the combined baryon-rich pt fluid, the evolution of the f fluid is separately presented in Fig. 2. The pt fluid entrains the f fluid. This is the reason for the smallness of v_{fB}.

As seen from Fig. 1, at $t = 1$ fm/c the matter of colliding nuclei has already partially passed though the interaction zone

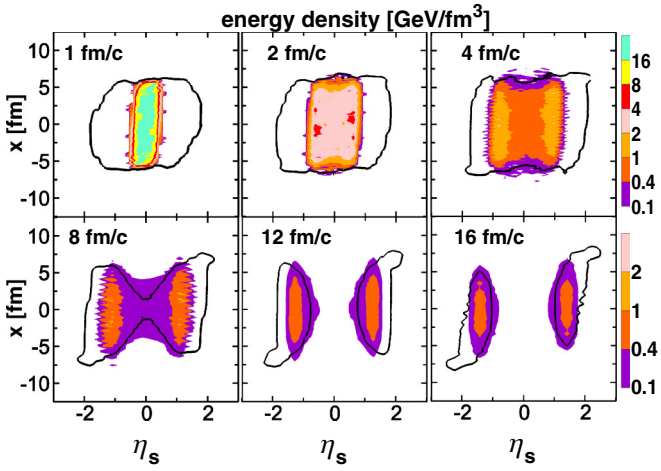

FIG. 2. Proper energy density of the baryon-free (f) fluid in the reaction plain (xz) at various time instants in the central ($b = 2$ fm) Au+Au collision at $\sqrt{s_{NN}} = 39$ GeV. Calculations are done with the first-order-transition EOS. The bold contours display the borders between the frozen-out and still hydrodynamically evolving matter.

(two bumps of baryon density near $\eta_s = \pm 1$) and has been partially stopped in the central region (the central bumps in n_B and ε). Thus, the central region and the fragmentation regions have already been formed to $t = 1$ fm/c. The matter in all these regions is in the quark-gluon phase, see the QGP fraction in Fig. 1. A large fraction of the baryon charge stopped in the central region ($\approx 70\%$) is in contrast to the ultrarelativistic scenario (at the top RHIC and LHC energies) where the major part of the baryon charge is assumed to be located in the fragmentation regions already at the initial stage. The proper baryon and energy densities in this central region approximately are $n_B/n_0 \approx 10$ and $\varepsilon \approx 40$ GeV/fm^3, respectively. The present situation is more similar to that at moderate energies, as predicted by transport models [21–25].

The fine structure of the evolving system along the beam axis ($\eta_s, x = y = 0$) is presented in Fig. 3. As seen, the central region undergoes a rapid, practically self-similar one-dimensional (1D) expansion right after its thermalization. This expansion pushes out the outer layers of the central fireball

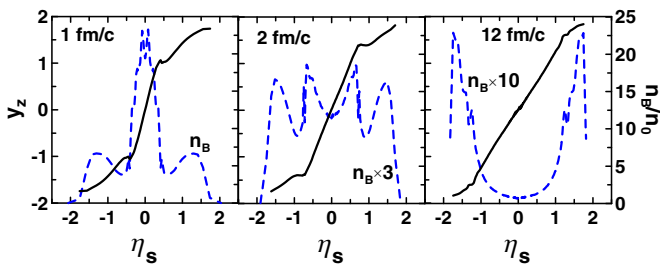

FIG. 3. Proper baryon density in units of the normal nuclear density (dashed lines, right scale axis) and the longitudinal rapidity (y_z) of the matter (solid lines, left scale axis) along the beam axis ($x = y = 0$) at various time instants in the central ($b = 2$ fm) Au+Au collision simulated within the first-order-transition scenario.

while the inner region serves as a driving force. The primordial fragmentation fireballs also expand in counter directions to the central one. The effect of this counter expansion is seen as wiggles in the η_s dependence of the longitudinal rapidity,

$$y_z = \frac{1}{2}\ln\left(\frac{1+v_z}{1-v_z}\right), \tag{6}$$

at the borders between the fragmentation and central fireballs, see $t = 1$ and 2 fm/c panels in Fig. 3. Here v_z is the z component of the hydrodynamical 3-velocity [Eq. (4)]. The positions of these wiggles precisely coincide with the borders between the f fluid and the primordial fragmentation fireballs, see Fig. 2.

In the course of time, this predominantly 1D expansion of the central fireball further proceeds, see Figs. 1 and 3. The matter, and in particular the baryon charge, is pushed out to the periphery of this central fireball, i.e., closer to the primordial fragmentation regions. The primordial fragmentation fireballs join with "central" contributions to the instant $t = 4$ fm/c because of their counter expansion, see Fig. 1. At $t = 12$ fm/c only tiny wiggles on the inner slopes of the density peaks and the corresponding tiny wiggles in the rapidity profile indicate this joining, see Fig. 3. Therefore, the final fragmentation regions consist of primordial fragmentation fireballs, i.e., the baryon-rich matter passed through the interaction region, and baryon-rich regions of the central fireball pushed out to peripheral rapidities. However, full mixing of these "central" and primordial fragmentation fireballs does not occur—the primordial fragmentation regions do not overlap with the f fluid even at late time instants, as seen from Fig. 2.

At later time $t \geqslant 10$ fm/c, see Fig. 1, the central part of the system gets frozen out while the fragmentation regions continue to evolve being already separated in the configuration space. This longer evolution of the fragmentation regions is due to the relativistic time dilation caused by their high-speed motion with respect to the central region. Therefore, their evolution time in the c.m. frame of colliding nuclei lasts ≈ 40 fm/c, as seen in Fig. 4.

To gain an impression of the proper baryon and energy densities attainable in a sizable volume, we present the evolution of mean proper densities averaged over the whole

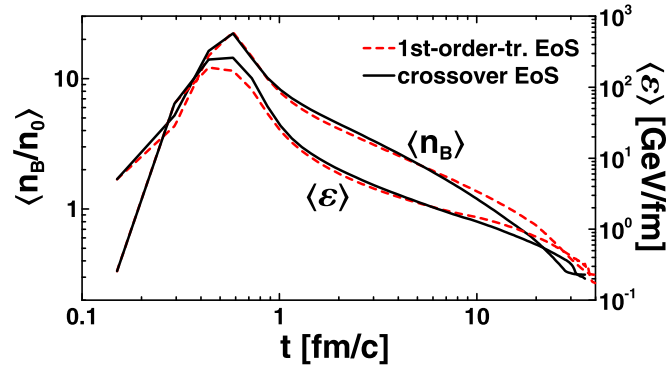

FIG. 4. Time evolution of the mean proper baryon (left scale) and energy (right scale) densities in central Au+Au collisions at $\sqrt{s_{NN}} =$ 39 GeV in simulations with different EOSs.

volume of a still hydrodynamically evolving system in Fig. 4. (Note that the freeze-out in the 3FD model removes the frozen-out matter from the hydrodynamical evolution [26].) These values are very similar for the first-order-transition and crossover EOSs. Note that this similarity is not due to similarity of these two EOSs. This similarity takes place because of the friction forces that were independently fitted for each EOS in order to reproduce observables in the midrapidity region.

In conclusion, it is demonstrated that at the initial thermalized stage of the central Au+Au collision, only $\approx 30\%$ of the baryon charge is located in fragmentation regions, while $\approx 70\%$ is- in the central fireball. The initial thermalized proper baryon and energy densities approximately are $n_B/n_0 \approx 10$ and $\varepsilon \approx 40$ GeV/fm^3, respectively. If the calculation is performed with the hadronic friction [17], we obtain a very high transparency of the colliding nuclei and at the same time do not reproduce the experimental data [20]. Therefore, the present results indicate that the transition into the QGP at the stage of interpenetration of colliding nuclei makes the system more opaque. Alternatively they may indicate a formation of strong color fields between the leading partons [5] preceding the QGP production. These fields may enhance baryon stopping as compared to its estimate based on hadronic cross sections [17].

Though these high densities are formed in the central fireball, their observable consequences manifest themselves in the fragmentation regions where this dense matter is pushed out by the subsequent fast 1D expansion of the central fireball along the beam direction. Thus, the final fragmentation regions in the central Au+Au collisions at $\sqrt{s_{NN}} = 39$ GeV are formed by not only primordial fragmentation fireballs, i.e., the baryon-rich matter passed through the interaction region, but also by the baryon-rich regions of the central fireball pushed out to peripheral rapidities. It is expected that the role of this central fireball gradually reduces with the collision energy rise and the dense baryon matter becomes predominantly located in the primordial fragmentation fireballs already at the initial stage of the collision.

This work was carried out using computing resources of the federal collective usage center complex for simulation and data processing for mega-science facilities at NRC "Kurchatov Institute," http://ckp.nrcki.ru/. Y.B.I. was supported by the Russian Science Foundation, Grant No. 17-12-01427. A.A.S. was partially supported by the Ministry of Education and Science of the Russian Federation within the Academic Excellence Project of the NRNU MEPhI under Contract No. 02.A03.21.0005.

[1] R. Anishetty, P. Koehler, and L. D. McLerran, Phys. Rev. D **22**, 2793 (1980).
[2] L. P. Csernai, Phys. Rev. D **29**, 1945 (1984).
[3] M. Gyulassy and L. P. Csernai, Nucl. Phys. A **460**, 723 (1986).
[4] L. Frankfurt and M. Strikman, Phys. Rev. Lett. **91**, 022301 (2003).
[5] I. N. Mishustin and J. I. Kapusta, Phys. Rev. Lett. **88**, 112501 (2002); I. N. Mishustin and K. A. Lyakhov, Phys. Rev. C **76**, 011603 (2007).
[6] S. J. Brodsky, F. Fleuret, C. Hadjidakis, and J. P. Lansberg, Phys. Rep. **522**, 239 (2013).
[7] M. Li and J. I. Kapusta, Phys. Rev. C **95**, 011901 (2017).
[8] L. D. McLerran and R. Venugopalan, Phys. Rev. D **49**, 3352 (1994).
[9] Yu. B. Ivanov, V. N. Russkikh, and V. D. Toneev, Phys. Rev. C **73**, 044904 (2006).
[10] Yu. B. Ivanov, Phys. Rev. C **87**, 064904 (2013).
[11] Yu. B. Ivanov, Phys. Lett. B **721**, 123 (2013); Yu. B. Ivanov and D. Blaschke, Phys. Rev. C **92**, 024916 (2015).
[12] Yu. B. Ivanov, Phys. Rev. C **87**, 064905 (2013).
[13] Yu. B. Ivanov, Phys. Rev. C **89**, 024903 (2014).
[14] Yu. B. Ivanov and A. A. Soldatov, Eur. Phys. J. A **52**, 10 (2016).
[15] Yu. B. Ivanov and A. A. Soldatov, Phys. Rev. C **91**, 024914 (2015); Yu. B. Ivanov, Phys. Lett. B **723**, 475 (2013).
[16] Yu. B. Ivanov and A. A. Soldatov, Phys. Rev. C (to be published) [arXiv:1801.01764].
[17] L. M. Satarov, Sov. J. Nucl. Phys. **52**, 264 (1990).
[18] V. M. Galitsky and I. N. Mishustin, Sov. J. Nucl. Phys. **29**, 181 (1979).
[19] A. S. Khvorostukhin, V. V. Skokov, K. Redlich, and V. D. Toneev, Eur. Phys. J. C **48**, 531 (2006).
[20] L. Adamczyk *et al.* (STAR Collaboration), Phys. Rev. C **96**, 044904 (2017).
[21] Y. Nara, N. Otuka, A. Ohnishi, K. Niita, and S. Chiba, Phys. Rev. C **61**, 024901 (1999).
[22] W. Cassing and E. L. Bratkovskaya, Nucl. Phys. A **831**, 215 (2009).
[23] S. A. Bass *et al.*, Prog. Part. Nucl. Phys. **41**, 255 (1998).
[24] N. S. Amelin and L. V. Bravina, Sov. J. Nucl. Phys. **51**, 133 (1990).
[25] Z. W. Lin, C. M. Ko, B. A. Li, B. Zhang, and S. Pal, Phys. Rev. C **72**, 064901 (2005).
[26] V. N. Russkikh and Yu. B. Ivanov, Phys. Rev. C **76**, 054907 (2007); Yu. B. Ivanov and V. N. Russkikh, Phys. At. Nucl. **72**, 1238 (2009).